J Mater Sci (2010) 45:2274–2284
DOI 10.1007/s10853-009-4152-x

Tensile behaviour of thermally bonded nonwoven structures: model description

Amit Rawal · Apurv Priyadarshi · Stepan V. Lomov · Ignaas Verpoest · Jozef Vankerrebrouck

Received: 6 November 2009 / Accepted: 18 December 2009 / Published online: 28 January 2010

Abstract Nonwovens are complex three-dimensional anisotropic structures and consisting of fibres orientated in certain directions, which are bonded by thermal, chemical, mechanical entanglement or a combination of these techniques. Thermally bonded are further classified in two categories, i.e. through-air and calendared nonwoven structures. In this study, a modified micromechanical model describing the tensile behaviour of thermally bonded nonwovens is proposed by incorporating the effect of fibre re-orientation during the deformation. The anisotropic behaviour of through-air bonded structures is demonstrated through theoretical stress–strain curves and the relationship between the fibre re-orientation and fabric strain is also analysed. Furthermore, the failure criterion of thermally bonded nonwovens is analysed using pull-out behaviour of fibres in the system. A parametric study revealing the dependencies of various structural and geometrical characteristics of fibres on pull-out behaviour of fibres in thermally bonded nonwovens is also discussed.

A. Rawal (✉) · A. Priyadarshi
Department of Textile Technology, Indian Institute of Technology Delhi, Hauz Khas, New Delhi, India
e-mail: arawal@textile.iitd.ac.in; amitrawal77@hotmail.com

S. V. Lomov · I. Verpoest
Department of Metallurgy and Material Engineering, Katholieke Universiteit Leuven, Kasteelpark Arenberg, 44, 3001 Leuven, Belgium

J. Vankerrebrouck
Libeltex bvba, Marialoopsteenweg 51, 8760 Meulebeke, Belgium

Introduction

Nonwovens are complex three-dimensional anisotropic structures and defined as fibres orientated in preferential or random directions and bonded by thermal, chemical, mechanical entanglement or a combination of these techniques. Thermally bonded nonwoven structures are produced by applying the heat energy to the thermoplastic component present in fibrous web and the polymer flows by surface tension and capillary action to form fused fibrous network. They are amongst the most widely used nonwovens, with applications ranging from baby diapers to high performance geotextiles. Thermal bonding can be further classified in two main types, i.e. calendar and through-air techniques. In calendaring, the fibrous web consisting of fibres oriented in certain directions is passed through high pressure heated rollers, whereas in through-air bonding the fibres are heated to the melting temperature of the binder fibres while moving through hot air oven. The latter is a highly useful technique in producing high bulk and heavyweight thermally bonded structures, which have good softness and drape characteristics [1]. Through-air and calendared bonded materials can be described as uncompressed and compressed fused fibrous networks, respectively. Knowledge of the relationship between microstructure and macroscopic properties is fundamentally important in determining the mechanical behaviour of such materials.

In general, the fibrous assemblies in the form of paper and nonwovens are anisotropic in nature and have similar structural characteristics except the fact that fibres can be bonded by means of hydrogen bonding in case of paper [2]. Therefore, various theories and mathematical models have been proposed for predicting the mechanical behaviour of fibrous assemblies such as nonwovens by both textile and

paper researchers. Cox [3] pioneered the approach of predicting the elastic behaviour of paper based on the distribution and mechanical characteristics of constituent fibres. The load transfer between the fibres has also been modelled using *shear-lag* theory. In shear-lag analysis, the embedded fibre in a matrix is subjected to a strain in the direction of fibre such that the rate of transfer of load will depend on the difference between displacements of fibre and matrix (without fibre) from the same reference point. Subsequently, Kallmes and his colleagues [4–7] extended Cox's model based on geometrical probability theory to determine fibre bonds, free fibre lengths between the contacts and their respective distributions for fibrous network in the form of paper. In addition, a theory was developed to predict the tensile strength of paper based on the fact that the local rupture of a fibre or bond failure is responsible for the total failure of sheet [8]. However, the usefulness of Cox approach has been disputed for simulated random fibre network and it has been revealed that the dominating mode of load transfer is through axial stress at the fibre intersections [9]. Nevertheless, the shear-lag model has been successfully applied to predict the tensile strength of paper by incorporating an important bond parameter, i.e. relative bonded area (fraction of fibre surface area occupied by bonds) [10]. The shear-lag mechanism has also formed the basis for transferring the load in representative volume element consisting of a fibre and portion of all crossing fibres and successfully computed the elastic–plastic behaviour of paper [11, 12].

On the other hand, the study of tensile deformation of nonwoven structure was pioneered by Backer and Petterson [13], and they applied well-known orthotropic theory for predicting the tensile properties of nonwovens. Moreover, the fibre network theory was also developed, and it was found suitable for nonwovens as it has included the effect of structural characteristics [13]. In fibre network theory, the fibre segments between the bonds are assumed to be straight, and the theory was further modified in order to include the effect of fibre curl or waviness [14, 15]. Parallel to these studies, van Wyk [16] calculated the number of fibre-to-fibre contacts, which is fundamentally important in determining the mechanical properties of fibrous assemblies. The theory was further *generalised* by computing the number of fibre contacts based on any fibre orientation distribution, length and arbitrary shape of the fibre cross-section [17, 18]. Pan [19] pointed out that the model for calculating the number of contacts deduced by Komori and Makashima [17] was incorrect as the probability of contact changes with successive contacts. Nevertheless, Pan et al. [20] employed a micromechanical approach in addition to continuum theory to compute the initial tensile response of two-dimensional hybrid fibrous structures. A three-dimensional micromechanical model has also been proposed based on the methodology of Cox [3] that predicted the initial response of dense anisotropic fibrous assemblies [21]. It was assumed that free fibre element is straight, and there is no slippage between the fibres in order to analyse the axial load bearing capacity of fibres. Since, it has been simulated earlier that fibre and bond extensions are primary modes of deformation in fibre networks in comparison to shear and bending deformations during tensile loading [22]. However, the micromechanical model was not validated experimentally. The tensile properties of nonwoven structures were also modelled using computer simulation techniques based on fictitious model of a nonwoven fabric, which was designed for mathematical convenience [23–25]. Furthermore, Grindstaff and Hansen [26] developed a two-dimensional computer model consisting of 30 bond points arranged in a 5 by 6 pattern for predicting the stress–strain properties of thermally point-bonded nonwoven structures. The input parameters included bond layout, fabric density, fibre orientation, fibre curl, fibre and bond tensile properties. The model can also incorporate the preferential orientation of fibres but the failure criterion of fibres in the thermally bonded nonwoven was highly intuitive in nature. For instance, when the samples are extended in the machine direction, fibre breakage at the interface was assumed to be the predominant failure mechanism, whereas fibre pull-out at a bond was considered as a failure criterion in the samples extended in the cross-machine direction. More recently, a force balance criterion is considered for computing the total force required against the force required to fail all the fibres [27]. A semiempirical model approach has also been applied to predict the strength of thermally point-bonded fabrics neglecting the fibre curl [28]. The effect of fibre curl along with orientation distribution has been recently incorporated in a modified micromechanical model for predicting the tensile behaviour of thermal bonded nonwoven structures assuming that there is no change in the orientation of fibre during the extension [29]. Alternatively, finite-element models have also been used for predicting the stress–strain characteristics of thermal bonded nonwovens [30]. It was indicated that the model can be potentially used for a wide variety of fibre orientation distributions yet the random orientation of fibres was considered in the finite-element model. Furthermore, the fibre rupture was assumed as a failure criterion in the model contrary to the previous experimental evidence that the failure in a thermally bonded structure occurs in the bond perimeter or at the interface between the bond and fibre [31, 32]. A Monte-Carlo simulation has also been applied for fibrous sheet consisting of defined layers of fibres orientated randomly for determining the tensile strength and elongation at break [33]. Poisson's ratio was assumed to be homogenous in nature, and it was noted that bonds started to break at 2–4% of elongation similar to the experimental results demonstrated using

environmental scanning electron microscope (ESEM) [34]. More recently, an analytical model for the load distribution along a fibre in a random nonwoven network has also been formulated [35]. The constituent fibres in a nonwoven network are assumed to be linearly elastic, and the forces developed at a particular contact point are functions of displacement and *stress transfer coefficient*. The *stress transfer coefficient* was determined either randomly or assigned as some constant value. There are several shortcomings of these theories/models before they can be applied to any nonwoven structure. First, most of the theories formulating three-dimensional models lack extensive experimental validation as it requires accurate measurement of out of plane fibre orientation angle and moreover, they are computationally unmanageable [11]. Similarly, the anisotropic characteristics in tensile properties of thermally bonded nonwoven structures also lack experimental validation [36]. Second, the fibre network theory and related models do not account for fibre re-orientation in order to compute the stress–strain characteristics of nonwoven structures. Finally, the failure criterion of nonwovens is generally dominated by fibre rupture in the literature. However, the fibre pull-out plays a key role in governing the fracture process and to determine the strength of thermal bonded nonwoven structures.

In the first part, the primary objectives is to modify the existing two-dimensional tensile model of thermally bonded nonwoven structures formulated by Rawal et al. [36] by incorporating the effect of fibre re-orientation during the tensile deformation. The failure criterion of thermal bonded structures has been determined by computing the maximum '*pull-out*' stress required for interfacial debonding between the fibre and bond. In the second part, the full tensile model would be validated for thermally bonded nonwovens including spunbonded structures, by determining the Poisson's ratio of the structures at various strain levels. The anisotropic behaviour of nonwoven structures under tensile mode of deformation would be further investigated using optical full field strain measurement technique. A comparison between the other theoretical models including fibre network theory and experimental results would be made in the successive part [14].

The organisation of the article is as follows: 'Theoretical' section describes the modification of existing tensile model by incorporating the fibre re-orientation in the model. It also focuses on the theoretical analysis of pull-out stress of fibres in through-air bonded nonwoven structures. 'Experimental' section presents the previous experimental work that has been carried out to understand the initial tensile response of through-air bonded nonwoven structures [36]. In 'Anisotropic behaviour of through-air bonded nonwoven structures' section, the anisotropic behaviour of through-air bonded structures is demonstrated through theoretical stress–strain curves, and the relationship between the fibre re-orientation and fabric strain is also analysed. 'Pull-out behaviour of fibres in through-air bonded nonwovens' section represents a parametric study revealing the dependencies of various structural and geometrical characteristics of fibres on pull-out stress in through-air bonded nonwovens, and finally conclusions are given in 'Conclusions' section.

Theoretical

Modified micromechanical model for thermal bonded nonwoven structures

In general, the following assumptions have been made in order to simplify the analysis.

- The structure consists of large number of fibres fused at the cross-over point, and it is homogenous in nature.
- The transfer of loads is mainly carried out by *heat* or *nonslippage* bonds and therefore, frictional characteristics between the fibres or the effect of *slippage* contacts have been neglected. Since, the *heat* or *nonslippage* bonds are stronger than the slippage contacts thus the load transfer is conceded through *nonslippage* bonds.
- Each fibre segment of microelement is straight before loading and therefore, local fibre curl or crimp is neglected. Since, the average bond–bond distance is considered to be small such that the fibre segment between the two successive bonds can be assumed as a straight line.
- Shear and bending deformations of the fibre segments are so small that they can be neglected. Since, it has been simulated earlier that fibre extension is the main deformation in fibre networks in comparison to shear and bending deformations during tensile loading [22].

Consider a microelement of average length $\bar{b}$ between the two bonds whose direction with respect to spherical coordinate system is defined by out of plane (θ) and in-plane (φ) fibre orientation angles, as shown in Fig. 1. Assuming, the fibre orientation distribution function, Ω, describing the probability of finding a fibre in the infinitesimal range of angle θ and $\theta + \mathrm{d}\theta$ and φ and $\varphi + \mathrm{d}\varphi$, is defined by $\Omega(\theta,\varphi)\sin\theta \mathrm{d}\theta\mathrm{d}\varphi$. However, the following normalisation condition must be satisfied:

$$\int_{\theta=0}^{\pi}\int_{\varphi=-\pi/2}^{\pi/2}\Omega(\theta,\varphi)\sin\theta \mathrm{d}\theta\mathrm{d}\varphi = 1 \quad (1)$$

According to Komori and Makashima [17] and Lee and Lee [37], the mean length of the fibre between the centre of

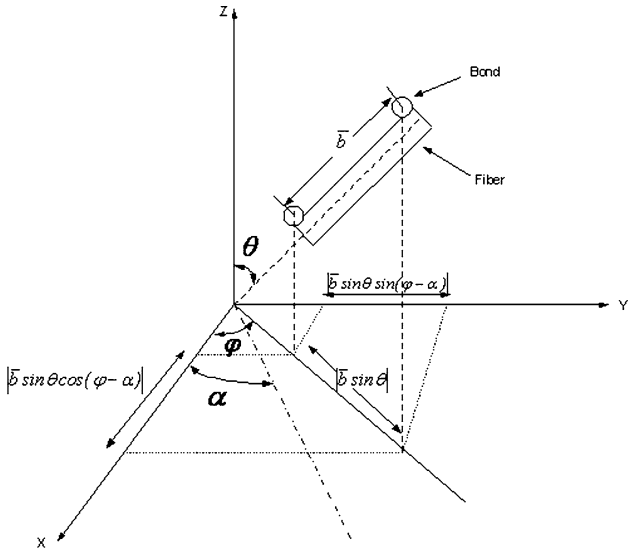

Fig. 1 Projection of fibre between two bonds

two neighbouring bonding points projected on the tensile test direction (α) be $\bar{b}_\alpha$ as shown in Fig. 1:

$$\bar{b}_\alpha = \bar{b}K_\alpha = \frac{V}{2DLI}K_\alpha, \tag{2}$$

$$I = \int_0^\pi \mathrm{d}\theta \int_0^\pi J(\theta,\varphi)\sin\theta\Omega(\theta,\varphi)\mathrm{d}\varphi, \tag{3}$$

$$J(\theta,\varphi) = \int_0^\pi \mathrm{d}\gamma \int_0^\pi \sin\chi(\theta,\varphi,\gamma,\zeta)\Omega(\gamma,\zeta)\sin\gamma\mathrm{d}\zeta, \tag{4}$$

$$\cos\chi = \cos\theta\cos\gamma + \sin\theta\sin\gamma\cos(\varphi-\zeta). \tag{5}$$

Also,

$$K_\alpha = \int_0^\pi \sin^2\theta\mathrm{d}\theta \int_{-\pi/2-\alpha}^{\pi/2-\alpha} |\cos(\varphi-\alpha)|\Omega(\theta,\varphi-\alpha)\mathrm{d}\varphi, \tag{6}$$

where D is the fibre diameter, L is the total length of the fibres in a volume V, K_α is the directional parameter or geometric coefficient when $\bar{b}$ is projected on the test direction and χ is the angle between the two axes of fibres having orientation distributions $\Omega(\theta,\varphi)$ and $\Omega(\gamma,\zeta)$.

In a 2D micromechanical model, assuming the fibres lying parallel to the XY plane (sheet-like assembly), i.e. $\theta = \pi/2$ such that Ω can be expressed using Dirac's delta function, i.e. $\Omega(\theta,\varphi) = \Omega_\varphi(\varphi)\cdot\delta(\theta-\pi/2)$ [17]. For a sheet-like assembly consisting of majority of fibres orientated in the machine or cross-machine direction (also known as preferential orientation of fibres), $\Omega_\varphi(\varphi)$ can be easily obtained from the experiments:

$$K_\alpha = \int_{-\pi/2-\alpha}^{\pi/2-\alpha} |\cos(\varphi-\alpha)|\Omega(\varphi-\alpha)\mathrm{d}\varphi. \tag{7}$$

Consider a mesodomain consisting of a fibre connected with the bonds at its ends and having a length of $\bar{b}_\alpha$ [20]. Without losing generality, the mesodomain is a constituent of a macroscopic volume, V, such that it has a unit cross-sectional area and volume, $\mathrm{d}V$ or $\bar{b}_\alpha$. Therefore, the number of bonds $n_{\mathrm{d}V}$ are calculated inside the volume $\mathrm{d}V$ assuming that the fibres are distributed uniformly in the space, and hence,

$$n_{\mathrm{d}V} = n\frac{\bar{b}_\alpha}{V}, \tag{8}$$

where n is the total number of bonds in the volume V, as shown below [17].

$$n = \frac{DL^2}{V}I. \tag{9}$$

In Eq. 9, it must be noted that Komori and Makashima [17] have not accounted for the change in the probability of contact with successive contacts, i.e. steric hindrance effect. Here, an existing contact reduces the effective contact length of a fibre, which reduces the probability of formation of new contacts. However, the existing fibre contact will also reduce the free volume of fibrous assembly leading to an increase in the chances of making new contacts [38]. Therefore, the effect of steric hindrance is contradictory in nature and may not have much relevance in computing the number of contacts per unit volume specifically for low fibre volume fraction-based nonwovens.

In addition, the total fibre length in the volume V is $L = N(V)\cdot l_\mathrm{f}$, where l_f is the average fibre length, and $N(V)$ is the total number of fibres in the volume V:

$$N(V) = \frac{V\cdot V_\mathrm{f}}{l_\mathrm{f}\frac{\pi D^2}{4}}. \tag{10}$$

Combining Eqs. 2, 8–10,

$$n_{\mathrm{d}V} = \frac{2V_\mathrm{f}}{\pi D^2}K_\alpha. \tag{11}$$

where V_f is the fibre volume fraction.

According to Rawal et al. [36], the stress in the sample can be computed as sum of tensile forces, experienced by the fibres connected by $n_{\mathrm{d}V}$ bonds based on the fact that each bond comprises two fibres. Thus, the stress in the fabric, $T(\alpha)$, can be calculated as follows:

$$T(\alpha) = mK_\alpha\sum_{j=1}^{n}\cos\beta_{ij}\chi(\beta_{ij})\sigma^\mathrm{f}(\beta_\mathrm{i},\bar{\varepsilon});\beta_\mathrm{i} = \varphi_\mathrm{i}-\alpha, \tag{12}$$

where m is the mass per unit area, $\chi(\beta_{ij})$ a frequency of j-th bin of a histogram, representing the distribution as a

function of the initial fibre orientation angle (β_i) and σ^f the fibre tensile stress.

Equation 12 can be extended for fused fibrous network containing n types of fibres, thus tensile stress can be calculated as follows:

$$T(\alpha) = \lambda_1 m K_{\alpha 1} \sum_{j=1}^{n} \cos\beta_{ij}\chi(\beta_{i1})\sigma_1^f(\beta_i,\bar{\varepsilon}) + \ldots + \lambda_n m K_{\alpha n} \sum_{j=1}^{n} \cos\beta_{ni}\chi(\beta_{in})\sigma_n^f(\beta_i,\bar{\varepsilon}) \quad (13)$$

where subscripts 1 and n refer to the components of the blend, $\bar{\varepsilon}$ the fabric strain, λ_1 and λ_n fractions of the components ($\lambda_1 + \cdots + \lambda_n = 1$).

In general, the constitutive model of fibre in tension is given by the following equation:

$$\sigma^f = f(\varepsilon_f) \quad (14)$$

where ε_f is the fibre strain.

According to Hearle and Stevenson [15], the strain exhibited by a fibre oriented at an initial angle β_i can be related to fabric strain by the following expression (see Fig. 2):

$$\varepsilon_f = \left(\cos^2\beta_i(1+\bar{\varepsilon})^2 + (1-\bar{\varepsilon}v)^2\sin^2\beta_i\right)^{1/2} - 1 \quad (15)$$

where v is the Poisson's ratio of the fabric in various test directions.

Equation 12 is modified by incorporating the effect of fibre re-orientation, as shown in Fig. 2, here fibre OB is aligned at an initial orientation angle, β_i, with respect to the loading or test direction. Under uniaxial loading, the upper end of the fibre moved from B to C and the orientation angle is changed to β_f, with respect to the loading or test direction. The re-orientation of the fibre can be related with the fabric strain, Poisson's ratio and initial fibre orientation angle by the following expression. The detailed mathematical treatment is presented in 'Appendix' section:

$$\beta_f = \cos^{-1}\left[\frac{(1+\bar{\varepsilon})}{\sqrt{(1+\bar{\varepsilon})^2 + \tan^2\beta_i(1-v\bar{\varepsilon})^2}}\right]. \quad (16)$$

Thus, the fabric stress, $T(\alpha)$, given in Eq. 12 can be calculated using modified relation in order to consider the effect of fibre re-orientation, as shown below:

$$T(\alpha) = mK_\alpha \sum_{j=1}^{n} \cos\beta_{fj}\chi(\beta_{fj})\sigma^f(\beta_f,\bar{\varepsilon}), \quad (17)$$

$$K_\alpha(\beta_f) = \int_{-\pi/2-\alpha}^{\pi/2-\alpha} |\cos(\beta_f)|\chi(\beta_f)\mathrm{d}\beta_f. \quad (18)$$

A Matlab® program was written to calculate the value of tensile stress in various test directions at different levels of strains.

Pull-out behaviour of fibres in through-air bonded nonwoven structures

In the past, experimental observations have pointed that that the failure in a thermal bonded structure occurs in the bond perimeter or at the interface between the bond and fibre [31, 34]. Thus, the pull-out behaviour of fibres in a thermally bonded nonwoven structure plays a key role in determining the failure criterion. According to Pan [39], the pull-out force for a single fibre can be calculated for a microelement consisting of two bonds of average length $\bar{b}$ and mean free fibre and bond lengths of $\bar{b}_f$ and $\bar{b}_b$, respectively, as shown in Fig. 3. Therefore, the maximum pull-out force (P_m) is given by Eq. 19 assuming that the fibre is fully embedded in the matrix or bond:

$$P_m = \frac{\tau_b w_b}{\rho}\tanh\rho\bar{b}_b. \quad (19)$$

Also,

$$\rho = \sqrt{\frac{G_b w_b}{E_f \pi r_f^2 t_b}}, \quad (20)$$

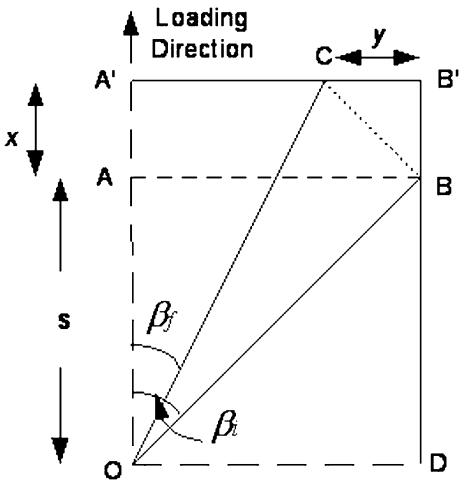

Fig. 2 Relationship between fibre and fabric strain

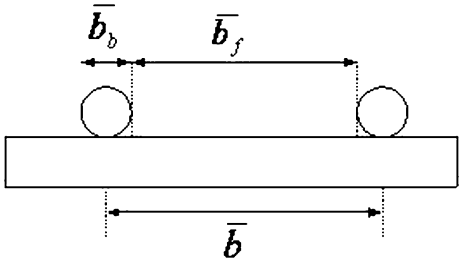

Fig. 3 A microelement

$$w_b = \sqrt{(\bar{b}_b - D)^2 + D^2}, \tag{21}$$

where w_b is the mean width of the bond, r_f is the radius of the fibre, D is the diameter of the fibre, $t_b(\approx 0.8r_f)$ is the thickness of the bond, E_f is the fibre modulus and G_b,τ_b are the shear modulus and shear strength of bond between the fibres, respectively.

As discussed earlier, consider a mesodomain consisting of a fibre connected with the bonds at its ends having a volume, dV. The total pull-out stress for mesodomain system consisting of n_{dV}, number of bonds in a volume, dV is given below:

$$P = \text{Int}(n_{dV})\frac{\tau_b w_b}{\rho}\tanh \rho\bar{b}_b \tag{22}$$

where Int() is the integer function, which omits the fractional part of the result as to indicate the discrete bonds.

From Eq. 11,

$$P = \text{Int}\left(\frac{2V_f}{\pi D^2}K_\alpha\right)\frac{\tau_b w_b}{\rho}\tanh \rho\bar{b}_b. \tag{23}$$

It is well known that fibres will be re-orientated in the loading direction due to the applied tensile strain, and therefore, the projection of fibre length needs to be updated, i.e. K_α will be replaced by $K_\alpha(\beta_f)$ in Eq. 23. Furthermore, the ratio of mean bond length to the mean length of the fibre between the centres of two neighbouring bonding points indicates the embedded length, i.e. $\frac{\bar{b}_b}{\bar{b}}$ needs to be incorporated in Eq. 23. Hence,

$$P = \text{Int}\left(\frac{2V_f}{\pi D^2}K_\alpha\frac{\bar{b}_b}{\bar{b}}\right)\frac{\tau_b w_b}{\rho}\tanh \rho\bar{b}_b. \tag{24}$$

Therefore, the maximum pull-out stress is obtained when bond length, $\frac{\bar{b}_b}{\bar{b}}$ approaches unity as shown below:

$$P_{max} = \text{Int}\left(\frac{2V_f}{\pi D^2}K_\alpha\right)\frac{\tau_b w_b}{\rho}\tanh \rho\bar{b}_b. \tag{25}$$

According to Pan [19], the overall mean bond dimension can be obtained by the following expression:

$$\bar{b}_b = DR. \tag{26}$$

Also,

$$R = \int_0^\pi \mathrm{d}\theta \int_0^\pi \Omega(\theta,\varphi)K(\theta,\varphi)\sin\theta \mathrm{d}\varphi \tag{27}$$

and

$$K(\theta,\varphi) = \int_0^\pi \mathrm{d}\gamma \int_0^\pi \Omega(\gamma,\zeta)\frac{\sin\gamma}{\sin\chi(\theta,\varphi,\gamma,\zeta)}\mathrm{d}\zeta, \tag{28}$$

where χ is the angle between the two axes of fibres having orientation distributions $\Omega(\theta,\varphi)$ and $\Omega(\gamma,\zeta)$.

In order to avoid the singular value of sin χ, the range of angle χ should range between the following limits,

$$\pi - \sin^{-1}\left(\frac{D}{l_f}\right) > \chi > \sin^{-1}\left(\frac{D}{l_f}\right). \tag{29}$$

In a 2D micromechanical model, assuming the fibres lying parallel to the XY plane (sheet-like assembly), i.e. $\theta = \pi/2$ such that Ω can be expressed using Dirac's delta function, i.e. $\Omega(\theta,\varphi) = \Omega_\varphi(\varphi)\cdot\delta(\theta - \pi/2)$ [17]. Furthermore, on applying the load, the fibres tend to move towards the loading direction. Therefore, the above expressions can be represented in terms of final fibre orientation angle (dependent upon fabric strain) as shown below:

$$\bar{b}_b = D\left\{\int_{-\pi/2-\alpha+\beta_f'}^{\pi/2-\alpha+\beta_f''}\frac{1}{|\sin(\beta_f)|}\chi(\beta_f)\mathrm{d}\beta_f\right\}. \tag{30}$$

Also

$$\beta_f'' > \beta_f > \beta_f' \tag{31}$$

where

$$\beta_f'' = \pi - \sin^{-1}\left(\frac{D}{l_f}\right) \tag{32}$$

and

$$\beta_f' = \sin^{-1}\left(\frac{D}{l_f}\right). \tag{33}$$

Moreover, the mean length of the fibre between the centres of two neighbouring bonding points projected on the test direction, i.e. $\bar{b}_\alpha$ can be calculated by following the approach of Komori and Makashima [17] and Lee and Lee [37]. In addition, the effect of fibre re-orientation has been considered as shown below:

$$\bar{b} = \frac{V}{2DLI} = \frac{\pi D}{8V_f I}. \tag{34}$$

The value of I can be obtained from Eq. 3, however, it can be deduced in 2D micromechanical model by using Dirac's delta function as shown below:

$$I(\beta_f) = \int_{-\pi/2-\alpha}^{\pi/2-\alpha}|\sin(\beta_f)|\chi(\beta_f)\mathrm{d}\beta_f. \tag{35}$$

Thus, pull-out stress can be obtained by combining Eqs. 24, 30 and 34, and iterations were performed for calculating the fibre orientation angle and its distribution at various levels of strains using Eq. 16.

Experimental

The reported work is based on two through-air bonded nonwoven structures, produced and supplied by the

company, i.e. Libeltex in the previous research work [36]. These structures were produced by blending the homofil (melting temperature: 250 °C) and bicomponent (core-sheath type with sheath melting temperature: 110 °C) polyester fibres in equal proportions by weight and labelled here as TB1 and TB2. These fibres were opened, blended and carded in the preferred direction, i.e. machine direction. In order to reduce the anisotropy, the fibres were randomised by means of random rollers similar to the process shown by Lin et al. [40]. Some of the important fabric and constituent fibre properties are given in Tables 1 and 2, respectively. Furthermore, the fibre orientation was measured by digitally capturing and analysing the images using optical microscope and LEICA QWIN software. The histograms of the relative frequency of fibres for 10° orientation angle interval with respect to the machine direction were computed to characterise the orientation distribution. Figure 4 shows the histograms of relative

Table 1 Properties of through-air bonded structures

Property	TB1	TB2	Source
Mass per unit area (g/m^2)	31.09	28.46	Rawal et al. [36]
Thickness (mm)	0.44 ± 0.0012	0.43 ± 0.0038	Rawal et al. [36]

Table 2 Properties of fibres used in the production of through-air bonded structures

Property	TB1		TB2		Source
Type of fibres	Polyester (homofil)	Polyester (bicomponent)	Polyester (homofil)	Polyester (bicomponent)	Rawal et al. [36]
Linear density (dtex)	2.2	3.3	4.4	12	Rawal et al. [36]
Length (mm)	48.83	58.38	47.8	61.22	Rawal et al. [36]
Diameter (μm)	14.9	18.3	21.1	34.9	Calculated

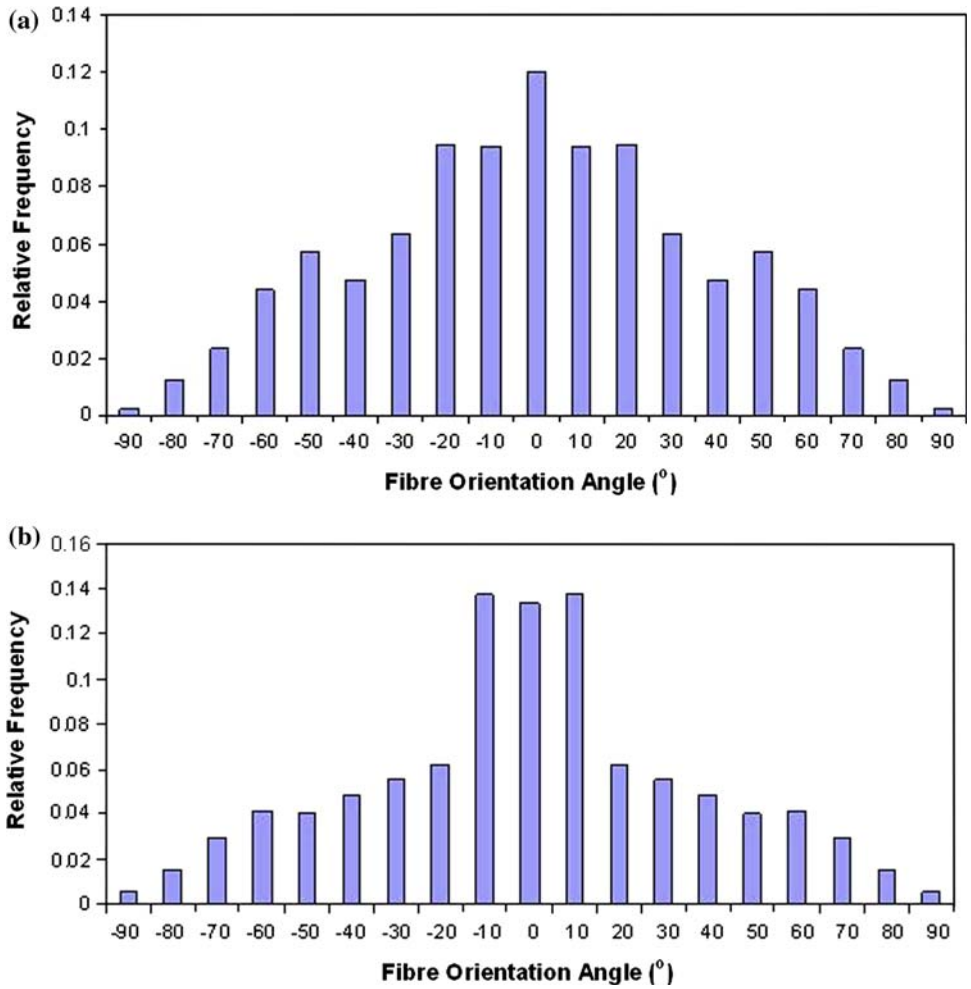

Fig. 4 In-plane fibre orientation distribution: **a** TB1 and **b** TB2

frequency of fibres that have been used in the production of thermal bonded nonwovens TB1 and TB2 (0° indicating the machine direction).

Anisotropic behaviour of through-air bonded nonwoven structures

Figure 5 shows the theoretical stress–strain curves of through-air bonded nonwoven structures, i.e. TB1 and TB2. The slope of stress–strain curves decreases with an increase in the angle of test direction. The results are also reflected in the fibre orientation distribution as shown in Fig. 4. Here, the effect of Poisson's ratio is not considered, however, the second part of the article will reveal the results of Poisson's ratio at various levels of strains using optical full field strain measurement technique.

Furthermore, a typical relationship between initial fibre orientation angle, fabric strain and final fibre orientation angle by neglecting the effect of fabric Poisson's ratio is shown in Fig. 6. It can be clearly seen that the initial load (up to 5% strain) is insufficient to re-orientate the fibres

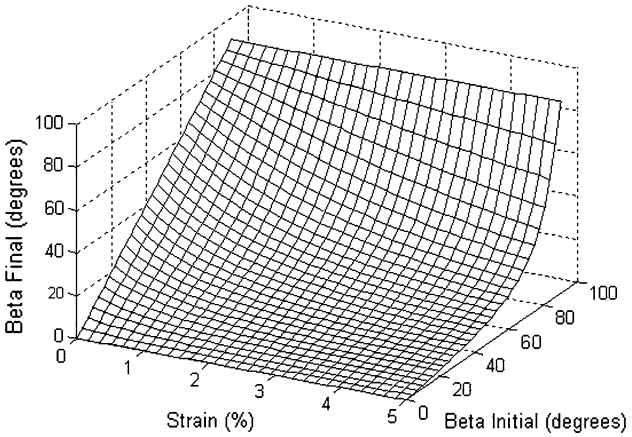

Fig. 6 Relationship between initial and final fibre orientation angles

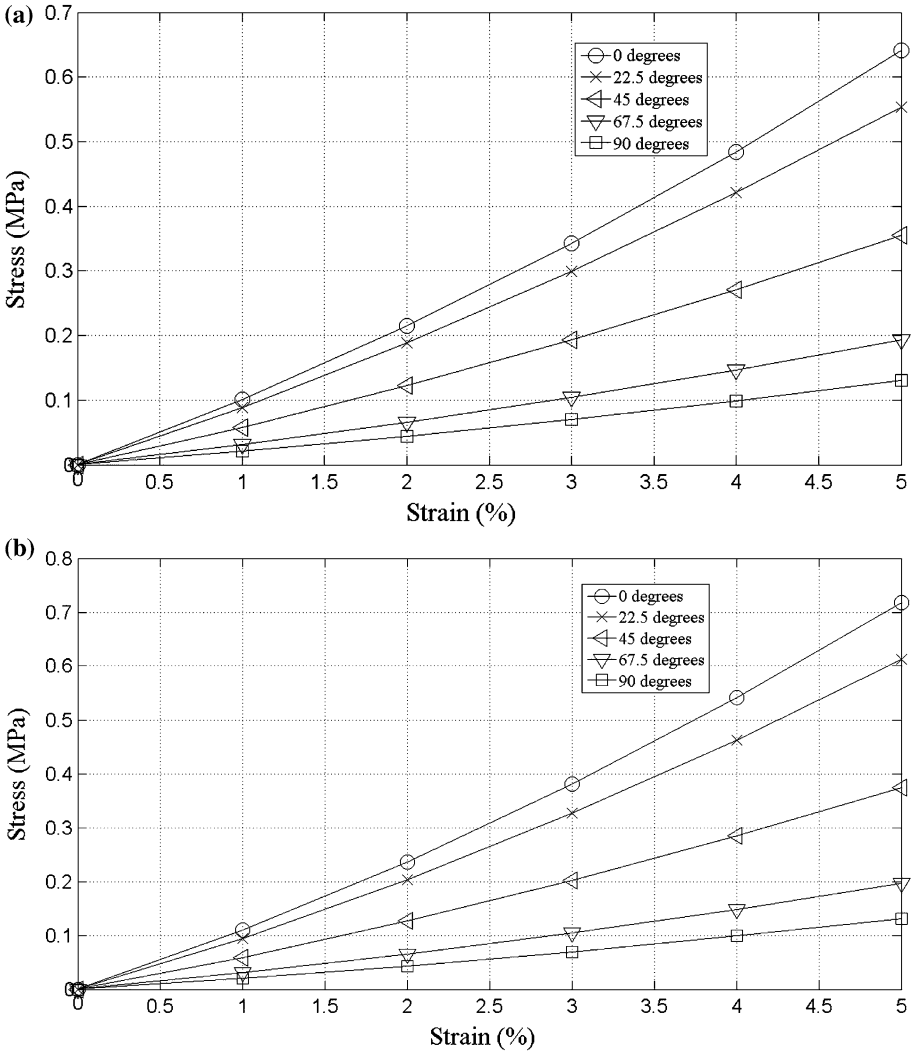

Fig. 5 Theoretical stress–strain curve: **a** TB1 and **b** TB2

orientated in the cross-machine direction (90°) towards the loading direction (0°). Here, beta final and beta initial denotes including and excluding the effect of fibre re-orientation, respectively. This result is similar to the experimental observations made through environmental scanning electron microscopy (ESEM) revealing that the fibres oriented in the loading direction are the load bearing elements, whereas the fibres lying perpendicular to the loading direction tend to break the bond followed by the small displacement in the loading direction (up to 5% strain) [34].

Pull-out behaviour of fibres in through-air bonded nonwovens

A parametric study demonstrating the effects of important structural and mechanical properties of constituent fibres on pull-out behaviour of fibres in through-air bonded nonwovens is shown in Figs. 7 and 8. These relationships are obtained using Eq. 24 and a fibre volume fraction calculated for TB1 and TB2 nonwovens, i.e. a value of 0.05, has been used for computing pull-out stresses at different embedded lengths. Figure 7 shows that an increase in the ratio $\frac{G_b}{E_f}$, i.e. a stiffer bond in shear or a lower fibre tensile modulus, results in a lower pull-out stress for the same embedded length. Thus, to better utilise the strength potential of the fibres, nonwovens with weak fibre–fibre bonds can yield in higher force to pull the fibres from the system. Furthermore, for the fibres that are randomly distributed in the system, the value of directional parameter (K_α) is found to be 0.63 using Eq. 7. Figure 8 shows that the randomly orientated fibres require lower pull-out stress in comparison to the anisotropic nonwoven structures for a given embedded fibre length. Since, the fibres orientated in a certain preferential direction tend to give more resistance than the randomly distributed fibres in the system.

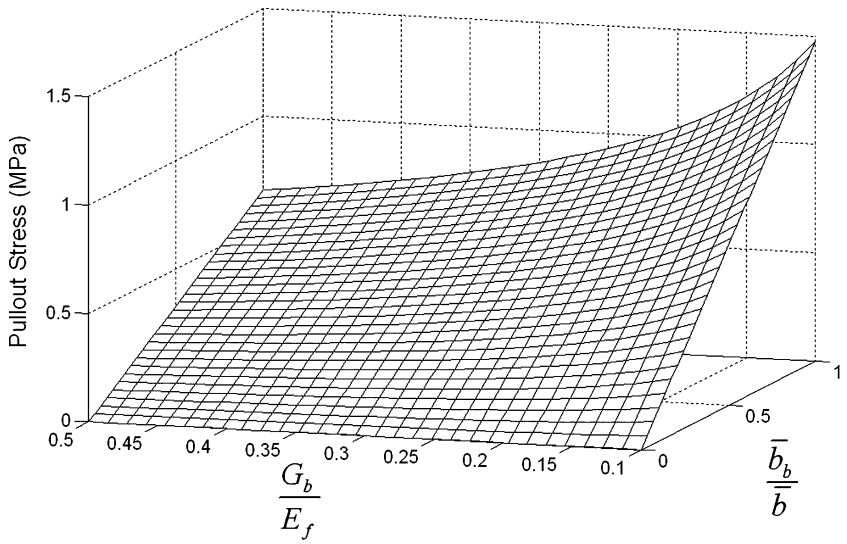

Fig. 7 Relationship between pull-out stress and ratio of bond shear modulus to fibre tensile modulus at different embedded fibre lengths

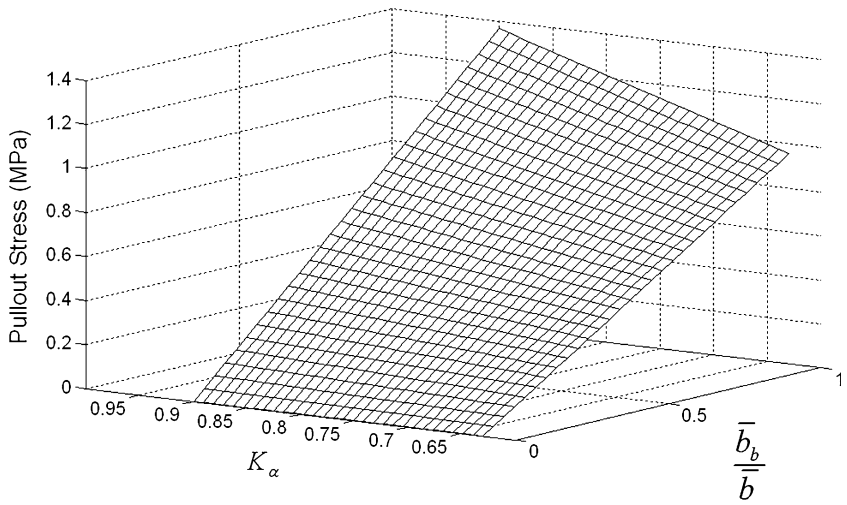

Fig. 8 Relationship between pull-out stress and directional parameter at different embedded fibre lengths (here the tensile modulus of the fibre is assumed to be 1 GPa)

Conclusions

The tensile behaviour is studied for through-air bonded nonwoven structures by incorporating the effect of fibre re-orientation in the existing model [36]. A relationship between initial fibre orientation angle, fabric strain and final fibre orientation angle has yielded that initial load is insufficient to re-orientate the fibres that are oriented perpendicular to the loading direction. The anisotropy in through-air bonded nonwovens has also been revealed through theoretical stress–strain curves. Since, the slope of the curves decreases with an increase in the angle of test direction and the tensile behaviour correlates well with the experimentally obtained fibre orientation distribution. The failure criterion of thermal bonded nonwoven is analysed using pull-out behaviour of fibres in the system. A parametric study of important structural and mechanical properties of constituent fibres on pull-out behaviour suggested that stiffer bond or randomly orientated structure can result in lower fibre pull-out stress.

Appendix

Figure 2 shows fibre OB aligned at an initial orientation angle, β_i, with respect to the loading or test direction. Under uniaxial loading, the upper end of the fibre is re-orientated to β_f, with respect to the loading or test direction:

$$\begin{aligned}&\text{Initial fabric length} = OA = s \quad \text{and}\\ &\text{Extended fabric length} = OA' = x + s,\end{aligned} \tag{36}$$

$$\text{Fabric strain } (\bar{\varepsilon}) = \frac{AA'}{OA} = \frac{x}{s}, \tag{37}$$

$$\text{Fabric Poisson's ratio } (v) = \frac{CB'/AB}{AA'/OA} = \frac{y/s\tan\beta_i}{x/s} = \frac{y}{x\tan\beta_i}$$

or

$$y = vx\tan\beta_i, \tag{38}$$

$$\text{Original fibre length} = OB = s/\cos\beta_i, \tag{39}$$

$$\text{Extended fibre length} = OC = \sqrt{OA'^2 + CA'^2} = \sqrt{OA'^2 + (AB - B'C)^2}$$

or

$$OC = \sqrt{(x+s)^2 + (s\tan\beta_i - y)^2}.$$

From Eq. 38,

$$OC = \sqrt{(x+s)^2 + (s\tan\beta_i - vx\tan\beta_i)^2}. \tag{40}$$

Also,

$$\cos\beta_f = \frac{OA'}{OC} = \frac{x+s}{\sqrt{(x+s)^2 + (s\tan\beta_i - vx\tan\beta_i)^2}}. \tag{41}$$

Dividing Eq. 41 by s and from Eq. 37,

$$\cos\beta_f = \frac{1+\bar{\varepsilon}}{\sqrt{(1+\bar{\varepsilon})^2 + \tan^2\beta_i(1 - v\bar{\varepsilon})^2}}. \tag{42}$$

References

1. Pourmohammadi A (2007) In: Russell SJ (ed) Handbook of nonwovens. Woodhead Publishing Ltd, England
2. Massenaux G (2003) In: Albrecht W, Fuchs H, Kittelmann W (eds) Nonwoven fabrics. WILEY-VCH Verlag GmbH & Co. KGaA, Weinheim
3. Cox HL (1952) Br J Appl Phys 3:72
4. Kallmes O (1972) In: Jayne BA (ed) Theory and design of wood and fiber composite materials. Syracuse University Press, New York
5. Kallmes O, Corte H (1960) TAPPI J 43:737
6. Kallmes O, Bernier G (1963) TAPPI J 46:108
7. Kallmes O, Corte H, Bernier G (1963) TAPPI J 46:493
8. Kallmes O, Bernier G, Perez M (1977) Paper Technol Ind 18:222
9. Raisanen VI, Alava MJ, Niskanen Nieminen RM (1997) J Mater Res 12:2725
10. Carlsson LA, Lindstorm T (2005) Compos Sci Technol 65:183
11. Ramasubramanian MK, Wang Y (2007) Int J Solids Struct 44(22):7615
12. Ramasubramanian MK, Perkins RW (1988) J Eng Mater Technol 110:117
13. Backer S, Petterson DR (1960) Textile Res J 30:704
14. Hearle JWS, Stevenson PJ (1963) Textile Res J 33:877
15. Hearle JWS, Stevenson PJ (1964) Textile Res J 34:181
16. van Wyk CM (1946) J Textile Inst 37:T285
17. Komori T, Makishima K (1977) Textile Res J 47:13
18. Komori T, Makishima K (1978) Textile Res J 48:309
19. Pan N (1993) Textile Res J 63:336
20. Pan N, Chen J, Seo M, Backer S (1997) Textile Res J 67:907
21. Narter MA, Batra SK, Buchanan DR (1999) Proc R Soc Lond A 455:3543
22. Hamlen RC (1991) Paper structure, mechanics and permeability: computer aided modeling. PhD dissertation, University of Minnesota
23. Britton PN, Sampson AJ, Elliott CF, Graben HW, Gettys WE (1983) Textile Res J 53:363
24. Britton PN, Sampson AJ, Gettys WE (1984) Textile Res J 54:1
25. Britton PN, Sampson AJ, Gettys WE (1984) Textile Res J 54:425
26. Grindstaff TH, Hansen SM (1986) Textile Res J 56:383
27. Kim HS, Pourdeyhimi B (2001) J Textile Appar Technol Manag 1:1
28. Erel S, Warner SB (2001) Textile Res J 71:22

29. Rawal A (2006) J Ind Textiles 36:133
30. Mueller DH (2004) Int Nonwovens J Spring:56
31. Dharmadhikary RK, Davis H, Gilmore TF, Batra SK (1999) Textile Res J 69:725
32. Gibson PE, McGill RL (1987) TAPPI J 70:86
33. Termonia Y (1997) Chem Eng Sci 52:3003
34. Rawal A, Lomov SV, Verpoest I (2008) J Textile Inst 99:235
35. Batchelor W (2008) Mech Mater 40:975
36. Rawal A, Lomov SV, Ngo T, Verpoest I, Vankerrebrouck J (2007) Textile Res J 77:417
37. Lee DH, Lee JK (1985) In: Kawabata S, Postle R, Niwa M (eds) Objective measurement: applications to product design and process control. The Textile Machinery Society of Japan, Osaka, pp 613–622
38. Pan N (1995) Textile Res J 65:618
39. Pan N (1993) J Textile Inst 84:472
40. Lin JH, Xu ZH, Lei CH, Lou CW (2003) Textile Res J 73:917